Francisco Branco Ferreira

Mestrado Integrado em Engenharia de Materiais

Novembro de 2017

Microstructural and Mechanical Characterization of Graphene Oxide-Reinforced Aluminium-Matrix Nanostructured Composites fabricated by Accumulative Roll Bonding

Dissertação para Obtenção do Grau de Mestre em Engenharia de Materiais

Orientador:	Doutor Alexandre Velhinho, Professor Auxiliar, Faculdade de Ciências e Tecnologia da Universidade Nova de Lisboa
Co-orientadora:	Doutora Isabel Ferreira, Professora Associada, Faculdade de Ciências e Tecnologia da Universidade Nova de Lisboa

Júri

Presidente:	Doutor Rui Silva, Professor Auxiliar, Faculdade de Ciências e Tecnologia da Universidade Nova de Lisboa
Arguente:	Doutor Telmo Santos, Professor Auxiliar, Faculdade de Ciências e Tecnologia da Universidade Nova de Lisboa

FACULDADE DE CIÊNCIAS E TECNOLOGIA
UNIVERSIDADE NOVA DE LISBOA

Microstructural and Mechanical Characterization of Graphene Oxide-Reinforced Aluminium-Matrix Nanostructured Composites fabricated by Accumulative Roll Bonding™

Acknowledgements

First of all I would like to thank my tutor, Professor Alexandre Velhinho, who since day 1 closely followed the progress of this work and was always available and willing to help me. Thank you for all the support and guidance!

Secondly, I would like to thank Faculdade de Ciências e Tecnologia da Universidade Nova de Lisboa (FCT-UNL) and all the DCM professors for all the knowledge and working methods that have been passed on during this course, in particular to Professor Rui Silva, Professor Francisco Brás Fernandes and especially to Professor Isabel Ferreira for her co-orientation on this work. Thank you for the availability and help through this dissertation!

I also want to thank Edgar Camacho for all the time he made available to help me whenever I came to "annoy" him at his office/lab.

Thanks also to Francisco Lopes, Ana Marques, Patrick Inácio and Daniela Gomes for all the help and contribution.

Finally, a big thank you to all my friends and family who directly or indirectly helped me overcome all the obstacles that a university course can bring, especially to my girlfriend Carolina Collinge, the person who most closely followed me along these years and was always present at the times I needed the most (thank you Carolina, you know what you mean to me!). And to my parents, António Ferreira e Otília Branco, for everything they taught me throughout my life, for everything they presented me with, for all the help and support, thank you!

Abstract

Accumulative Roll Bonding (ARB) was used to fabricate Graphene Oxide-reinforced Al-matrix composites, benefiting from a grain refinement effect of the metallic matrix.

Graphene Oxide reinforcement was suspended in a stabilized aqueous solution and applied, prior to each ARB cycle, through airgun spraying, in order to obtain a homogeneous distribution. Concentrations of 0.5, 2.5 and 10 mg/ml (graphene oxide/millipore water) were used. For each concentration, samples produced have undergone up to 5 rolling cycles.

Optical and electron scanning microscopies were used for microstructural characterization of the rolled composites which revealed a non-homogenous deformation of the layers across the composite's thickness. Although not desired but expected, Aluminium oxide formation occurred where the reinforcement was applied.

Although the presence of graphene-oxide promoted an increase in the microhardness, higher values were obtained with its lowest concentration for the same number of ARB cycles. The number of ARB cycles and the direction of the tested sections also influenced the microhardness results since the 5-cycle samples and the rolling direction sections for all the samples achieved higher hardness results. Graphene Oxide revealed to be a major contributor to the increase of stiffness during bending of the tested samples.

The ARB processed samples revealed a decrease on the electrical conductivity when compared with the annealed Aluminium, since the Graphene Oxide and Aluminium oxide have insulator properties. The contribution of the reinforcement to this decrease was only noticeable when using higher concentrations, since the sample with less concentration of the applied Graphene Oxide revealed slightly better results than the sample without any reinforcement.

Keywords: Accumulative Roll Bonding (ARB); Metal-Matrix Composite (MMC); Graphene-Oxide (GO); Grain Refinement.

Resumo

A técnica de *Accumulative Roll Bonding* (ARB) foi utilizada para fabricar compósitos de matriz de Alumínio reforçado com óxido de grafeno, beneficiando de um efeito de refinação de grão da matriz metálica.

O óxido de grafeno foi suspenso numa solução aquosa estabilizada e aplicado, antes de cada ciclo ARB, através de pulverização de uma pistola de ar comprimido, de modo a obter uma distribuição o mais homogénea possível. Foram utilizadas concentrações de 0,5, 2,5 e 10 mg / ml (óxido de grafeno / água *millipore*). Para cada concentração, as amostras produzidas sofreram até 5 ciclos de ARB.

Foram utilizadas microscopias óptica e electrónica de varrimento para a caracterização microestrutural dos compósitos laminados que revelaram uma deformação não homogénea das camadas em toda a espessura do compósito. Embora não desejado, mas esperado, a formação de óxido de alumínio ocorreu onde o reforço foi aplicado.

Embora a presença do óxido de grafeno tenha promovido um aumento da microdureza, os valores mais elevados foram obtidos para as amostras com a menor concentração, para o mesmo número de ciclos de ARB. O número de ciclos de ARB e a direcção das seções testadas também influenciaram os resultados de microdureza, uma vez que as amostras de 5 ciclos e as secções da direcção de rolamento para todas as amostras atingiram resultados de dureza mais elevados. O óxido de grafeno revelou ser um dos principais contribuintes para o aumento da rigidez durante a flexão das amostras testadas.

As amostras processadas por ARB revelaram uma diminuição da condutividade eléctrica quando comparadas com o alumínio recozido, uma vez que o óxido de grafeno e o óxido de alumínio possuem propriedades isoladoras. A contribuição do reforço para esta diminuição foi apenas perceptível quando se utilizaram concentrações mais elevadas, uma vez que a amostra com menos concentração do óxido de grafeno aplicado revelou resultados ligeiramente melhores do que a amostra sem reforço.

Palavras-chave: *Accumulative Roll Bonding* (ARB); Compósito de Matriz Metálica; Óxido de Grafeno; Refinamento de Grão.

Contents

List of Tables

List of Figures

Acronyms

ARB – Accumulative Roll Bonding

GO – Graphene Oxide

MMC – Metal Matrix Composite

UFG – Ultra.fine Grain

SPD – Severe Plastic Deformation

CVD – Chemical Vapour Deposition

rGO – Reduced Graphene Oxide

Rpm – Rotations per minute

OM – Optical Microscope

SEM – Scanning Electron Microscope

HNO_3 – Nitric Acid

HCl – Hydrochloric Acid

HF – Hydrofluoric Acid

RD – Rolling Direction

TD – Transverse Direction

EDS – Energy Dispersive X-Ray

IACS – International Annealed Copper Standard

E_B – Stiffness Modulus during Bending

σ_y – Yield Strenght

F – Applied Force

L – Length of Support Span

W – Width of the Sample

D – Maximum Centre Deflection/ Maximum Stroke

t – Thickness of the Sample

I – Current

V – Voltage

ρ – Electrical Resistivity

s – Probe Spacing

F (t/s) – Geometrical Factor used in the 4 point probe resistivity test

1 Introduction

1.1 Composites

Composites and their use have been a major subject of investigation in recent decades with an aim pursuing a lightweight, hard and more resistant material while also retaining a good performance at high temperatures [1].

Metals and its alloys cannot simultaneously achieve the desired properties in terms of strength and stiffness in various applications, wherefore it has become necessary to develop Metal Matrix Composites (MMCs). The composites' ductility is provided by the metal matrix and the stiffness by the reinforcement, generally constituted by particles, monofilaments or fibres of a ceramic material [1].

The most conventional techniques for the production of MMCs are casting and powder metallurgy, however, they hold some drawbacks such as the production cost and imperfections like porosities and agglomeration of the reinforcements which lead to a low homogeneity affecting the mechanical and electrical properties of the composite. In order to reduce these disadvantages, this work focuses on an alternative technique, Accumulative Roll Bonding (ARB), which in addition to the composite production allows a significant reduction of the matrix grain size, fitting in the field of Ultra-Fine Grain (UFG) materials [2].

1.2 Accumulative Roll Bonding

Several investigators have focused their study on UFG materials since these undergo several changes to their microstructures. Such materials have great potential to improve mechanical properties, therefore increasing the possible applications of cheap and lightweight metals such as aluminium. At room temperature UFG materials present excellent strength and, if the grains are fairly stable, exhibit impressive superplastic properties at elevated temperatures [3].

In order to obtain this grain size, several Severe Plastic Deformation (SPD) techniques can be used. In this work we used the ARB technique which is a simple, contin-

uous and low-cost process with a high productivity, reducing also the defects caused by porosities, agglomerates and low wettability of the reinforcements. These vast advantages make ARB the most applied technique in the manufacture of UFG metal sheets [4, 5].

At the macroscopic level, the ARB process is similar to a classic rolling, however, differences occur at the microscopic level which relate to the degrees of freedom which are available for the plastic deformation of individual grains.

ARB consists of a repeated stacking and hot roll bonding process of two strips. The initial strip is divided into two and both strips are surface-treated to remove impurities and oily residues which hinder the rolling process. The strips are stacked, heated and go through rolling mills whose opening is equivalent to the thickness of one strip which provides a 50% reduction of the laminated strip thickness. Both rollers speed is equal but rotate in opposite directions, as can be seen in the following representative diagram of the process cycle in Fig.1.1:

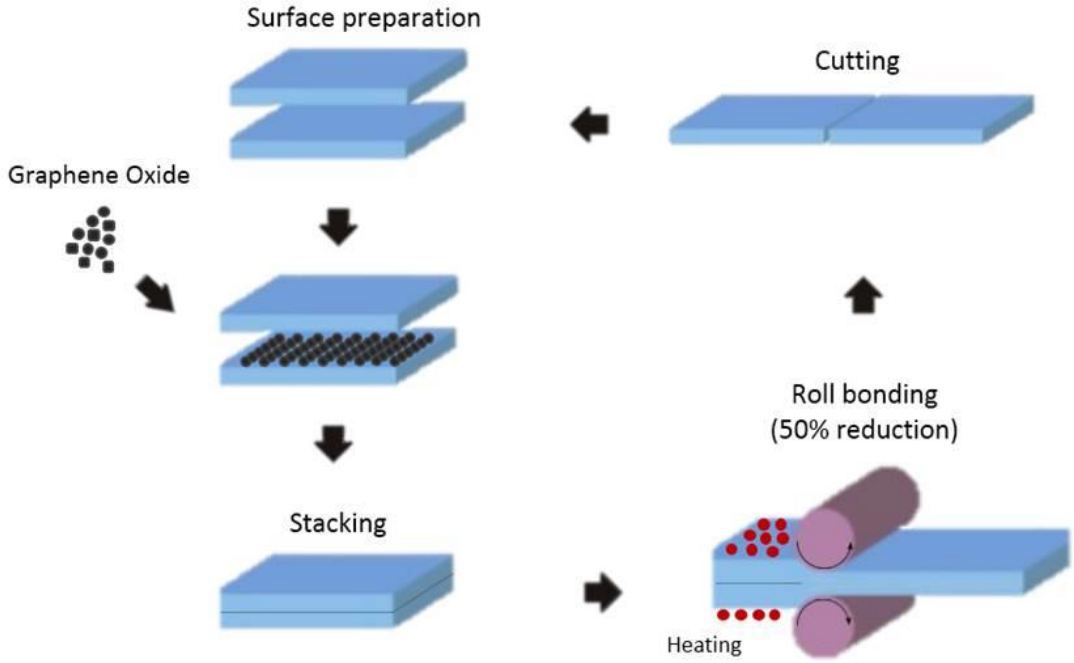

Fig.1.1: Representative diagram of ARB process using graphene oxide as reinforcement (adapted from [2]).

Due to high friction conditions between the sample and the roll, deformation can occur especially alongside the surface which results in an uneven distribution of the shear stress throughout its thickness. As such, and for the entire thickness to obtain the

ultrafine grain size, six ARB cycles are required which lead to a shear stress homogenization through the sample thickness [6].

Grain refinement occurs in a direction perpendicular to the surface which generates an anisotropic material. In the remaining directions, there is an increase in grain size which is readily observable by its length increase (very significant) and width (less significant). In spite of the high stresses applied and consequent refinement of the material, its cross-section does not suffer any significant changes with the various layers being visible under an optical microscope [2, 4].

Through each cycle and prior to the rolling process, reinforcement may be introduced. These reinforcements used in ARB can be sheets, fibres or particles.

Particles deposition becomes a challenge as its distribution must be homogeneous and free from irregularities and agglomerates wherefore this step must be carefully carried out. In order to ease an even deposition of the particles, these are usually suspended in a solution. At an industrial level the suspension solution is deposited by airgun spraying, guaranteeing the high quality of the process [2, 7].

1.3 Graphene/ Graphene Oxide

The Carbon element due to its versatility is considered the structural unit base of organic chemistry. Depending on formation conditions it can present various allotropic forms: diamond, fullerenes, nanotubes, graphite and graphene[8].

Indeed, in its early stages of investigation, the use of graphene as a reinforcement for MMC seems to have a great value thanks to its outstanding intrinsic properties, such as high Young's modulus (1 TPa), fracture strength (125 Gpa), high thermal conductivity (5000 Wm-1 K-1) and charge-carrier mobility (200,000 cm2 V-1 s-1) [8–10].

Graphene synthesis can be achieved by two different approaches, top-down and bottom-up. While the first involves the separation of the stacked layers of graphite to produce individual graphene sheets or small stacks, the bottom-up methods involve synthesizing graphene from simple carbon molecules such as methane and ethanol. Both approaches are shown in Fig.1.2 as a schematic illustration [11].

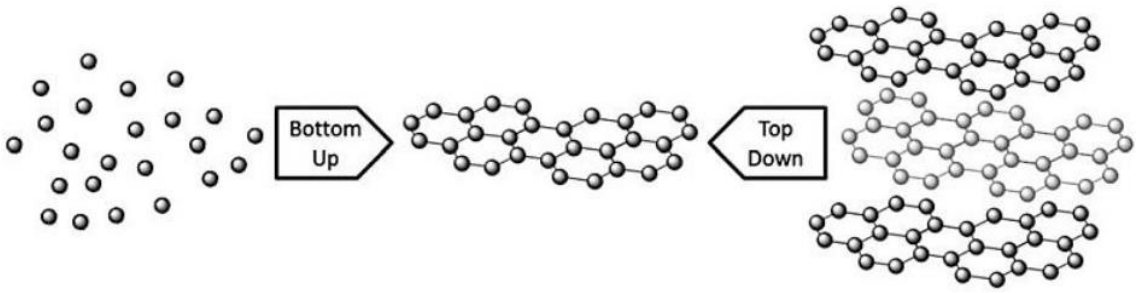

Fig.1.2: Representative scheme of the top-down and bottom-up approaches of the graphene synthesis [11]..

Epitaxial growth on Sic substrates and chemical vapour deposition (CVD) are part of bottom-up methods while mechanic exfoliation and exfoliation by chemical oxidation followed by reduction of graphene by-products, such as graphene oxide, are part of top-down methods [12]. Although the CVD method seems to be the ideal approach, in addition to the need to use substrates such as Si, Ni or Cu, high temperatures are required and it has a low yield [13].

Bottom-up methods may result in less defective graphene which, although is a key factor in the electronics field, are not applicable in composites since these require large amounts of material. As for the top-down methods, these are evaluated as best when applied to the production of graphene for its low cost and high yield. However, graphene use still has some way to go since process control, large-scale production and reproducibility remain challenging [14, 15].

Chemically synthesised graphene is obtained through two main steps. First, the mixing of the graphite with strong oxidants and exfoliation, via ultrasound, to obtain GO, and secondly reducing the GO by chemical or thermal reduction obtaining rGO [14].

Several conditions and reagents for the oxidation of graphite are studied. These can be classified as Chlorate based methods which were developed by Brodie, Staudenmaier and Hofmann, or Permanganate based methods, studied by Hummers and Offeman having small variations [16].

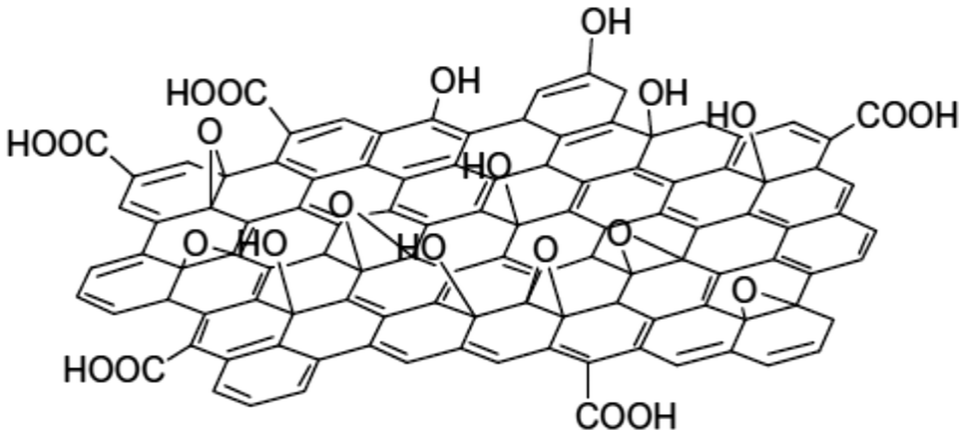

Fig.1.3: Representation of the probable functional groups present in the GO structure [17].

Chemically similar to oxidised graphite, GO consists of graphite structures composed by a functionalized layer of graphene with epoxy, hydroxyl, carboxylic and carbonyl groups. It is usually prepared by the oxidation of graphite flakes giving hydrophilic and dispersive characteristics to the GO turning it compatible with various polymeric matrices [11].

However, the amount, type and location of the functional groups may vary according to the synthesis conditions. A representation of probable functional groups present in the GO structure is illustrated in Fig.1.3. Since the GO properties are associated with the nature of the functional groups and the morphology of the obtained oxide, these characteristics depend on the initial graphite and the reaction conditions such as oxidation time, temperature and oxidation agents, which strongly influences the reactivity of these materials [18].

Although increasing the number of oxygen-containing groups improves the GO aqueous dispersity, it also increases structure defects making it electrically insulated. In order to restore conductivity, the GO functional groups should be removed by means of reduction [14, 15].

In this work we used graphene oxide (GO) instead of graphene as a reinforcement which do not guarantee the same final properties of the material but it is easier to deposit, handling and produce.

This dissertation is focused on two main objectives: to produce an Aluminium/GO MMC from a pre-treated aluminium sheet using the ARB process and to characterize the composite's microstructure, mechanical properties and its electrical conductivity.

2 Materials and Experimental Procedures

2.1 Materials

A commercial Aluminium sheet was cut into 100×50 ×0.8 mm^3 individual strips and these were annealed at 500 ºC for 2 h in order to homogenize the microstructure and defuse any residual stresses present in the sheet material prior to any ARB process.

As reinforcement, GO was synthesized from pyrolytic graphite (a waste of the high temperature furnaces of the metallurgy industry) using the modified Hummers method as described elsewhere [19]. Briefly, 4 g of pyrolytic graphite powder were mixed together with 2 g of sodium nitrate in 92 ml of sulphuric acid. After 1 h, 12 g of potassium permanganate were added slowly and stirred for 12 h before the addition of 2 l of water and 20 ml of hydrogen peroxide. The suspension was washed with hydrochloric acid and water by filtration. The final GO powder was obtained by freeze drying for 48 h. Concentrations of 0.5, 2.5 and 10 mg/ml (graphene oxide/millipore water) were used and ultrasonic exfoliation was carried out in an ice bath for 4h, with ON/OFF intervals of 1 minute each.

2.2 ARB Processing

The ARB processing diagram is illustrated in Fig.1. Prior to each ARB cycle, the surfaces of the annealed strips were prepared. This preparation consisted of wire brushing with a stainless steel brush in order to remove the oxide film caused by the annealing and to increase friction between the strips, followed by a degreasing ultra-sonic cleaning in alcohol and acetone baths, respectively, for 720 s each. At this point the graphene oxide suspension was applied by airgun-spraying and both strips were stacked and tied with an Alumel (95% Ni, 5% Al) wire at both ends to ensure that the strips don’t slide during the rolling process. The stacked strips were heated for 15 minutes at 550 ºC to alleviate stresses. A laboratory rolling mill was used for the ARB process consisting of two 75 mm diameter rolls at 13rpm and no lubricant was used in any ARB cycle. The distance between rolls was equal to the thickness of one strip, 0.8 mm, result-

ing on a 50% thickness reduction after each cycle. The rolled strip was then cut in half and stacked again after cleaning its surface. This process was repeated up to 5 ARB cycles for each GO concentration. The initial solution concentration does not directly reflect on the material concentration deposited on the composite which is subject to local variations. Moreover, the required operation speed for the ARB process prevents the determination of the effective concentration. One sample prepared without any reinforcement and with 4 ARB cycles was used for comparison purposes.

2.3 Microstructure Characterization

To analyse the microstructure, optical (OM, Leica DMI5000 M) and scanning electron microscopies (SEM, Zeiss Auriga) were used. To identify the presence of the GO reinforcement and its distribution, Raman spectroscopy (WITec Alpha 300 RAS) was performed at room temperature using a 30 mW green laser with excitation wavelength of 532 nm.

Prior to any characterization the samples were prepared according to a conventional metallography method, being grinded and polished up to P4000 sandpaper followed by 1/2 µm and 1/4 µm diamond slurry (Amplex Diamix) using an automatic polisher (Presi Mecatech 334) and etched with Keller's reagent (5 ml 65% HNO_3, 3 ml 37% HCl and 2 ml 48% HF in 190 ml distilled water) for 20 s. Both rolling direction (RD) and transverse direction (TD) sections were observed. For each concentration, the tested samples had gone through 4 and 5 ARB cycles.

2.4 Mechanical Tests

2.4.1 Microhardness Testing

For the microhardness measurement, a Vickers microhardness tester (ZWICK/ROELL) was used. All tests were carried out with a load of 1 kg (HV1) and a dwell time of 15 s.

Hardness profiles were performed along the thickness of the sample, with the number of measurement points being equal to 2n, where n is the number of ARB cycles,

meaning that there is one measurement point for each layer, with each point being equi-distant from each other, and each one follows the diagonal of the section. Both RD and TD sections were tested. For each concentration, the tested samples went through 4 or 5 cycles.

There were two identical samples for each concentration and the measurements were repeated to guarantee the accuracy of the results. An annealed Al sample was tested for comparison purposes.

2.4.2 Three-point bending test

In order to evaluate the stiffness modulus during bending E_B and yield strength σ_y of the samples several static three-point bending tests were carried using a standard universal testing machine with a 500 N load cell at a crosshead speed 5 mm mm^{-1}.

E_B of the samples was measured following to Eq.(1) after the bending tests (ASTM D5934-02) [20]:

$$E_B = \frac{FL^3}{4WDt^3} \text{ (GPa)} \quad (1)$$

where F, L, W, D and t are the applied force (N), the length of support span (mm), the width of the sample (mm), the maximum centre deflection/ maximum stroke (mm) and the thickness of the sample (mm), respectively.

Also, Yield Stress was evaluated through Eq. (2) by considering the onset of inelastic behaviour during bending:

$$\sigma_B = \frac{3FL}{2Wt^2} \text{ (MPa)} \quad (2)$$

The length of the support span was 30 mm for all the tested samples except the 4-cycle ARB, without GO reinforcement, which had a 20 mm length due to its dimension limitations. An annealed Al sample was tested for comparison purposes.

2.5 Electrical Conductivity Testing

Electrical conductivity characterization was conducted by two different tests: Eddy Current and 4 point probe.

The Eddy Current test (OLYMPUS NORTEC 500C) is a simple and quick test based on induced currents and the results are obtained in % IACS (International Annealed Copper Standard). This unit uses the copper conductivity as a reference (% 100 IACS).

For the 4 point probe (JANDEL) resistivity measurements a fixed 0.08 A current (I) was applied and voltage was measured 20 times for each test of each sample. The data were only considered once the voltage (V) results became constant (linear form).

The calculated resistivity (ρ) is dependent on the thickness of the samples (t). The probe spacing (s) was 0.635 mm. If ($t > 2.5*s$) the resistivity follows Eq. (2):

$$\rho = 2\pi\, s\, \left(\frac{V}{I}\right) \tag{2}$$

If (0.4 < (t/s) < 1.6666) the resistivity values follow Eq. (3) [21] where F (t/s) is a geometrical factor and presented in Table 6.1.

$$\rho = \frac{V}{I} \cdot t \cdot \frac{\pi}{ln2} \cdot F\left(\frac{t}{s}\right) \tag{3}$$

Like the microhardness and the three-point bending tests, an annealed Al sample was tested for comparison purposes. Prior to the testing the superficial oxide layer was removed by using sandpaper (this step has a greater importance in the 4 point probe resistivity measurements). In both tests and for each sample, measurements were taken three times in order to minimize the error.

3 Results and Discussions

In this chapter the results obtained in the various tests carried out on ARB processed composites will be exposed and discussed. The order in which they will be discussed is arranged with a first phase of analysis of their microstructure (OM, SEM and Raman spectroscopy) and, at a later stage, mechanical (microhardness, three point bending) and electrical conductivity (Eddy current, 4 point probe) tests will be discussed and different samples (number of ARB cycles, reinforcement concentrations) will be compared.

3.1 Microstructure Characterization

3.1.1 Optical Microscope

Bright field optical micrographs can be observed in Fig.3.1. The interface lines between layers can be observed in all of the samples, which either means that the adhesion is not perfect across the section or that the GO is present in those interface lines, although there are regions where the Al-Al interface exists, resulting in a fading of those lines. This can be explained by a possible non-homogeneous distribution of the GO reinforcement when applied or an aluminium dragging caused by the grinding and polishing process. Micrographs (a) and (b) correspond to the same 4-cycle ARB sample whereas (c) and (d) correspond to the same 5-cycle ARB sample. By comparing micrograph (a) and (b), which correspond to a periphery layer and a middle layer respectively, there is a significant difference in the thickness of the layers (70 µm and 130 µm, respectively). This means that for this number of cycles (4) the grain refinement is not homogenous through all the layers. Layers closer to the surface suffered higher deformation due to high friction conditions between the sample and the roll. Micrograph (c) shows one of the periphery layers and (d) shows one of the middle layers. The difference between the thickness of these layers is smaller (47.4 µm and 60.7 µm, respectively), showing that grain refinement is more homogenous through the thickness of all layers in a 5-cycle ARB than a 4-cycle ARB. As the number of ARB cycles increase, the thickness of all layers is expected to become similar across the sample section.

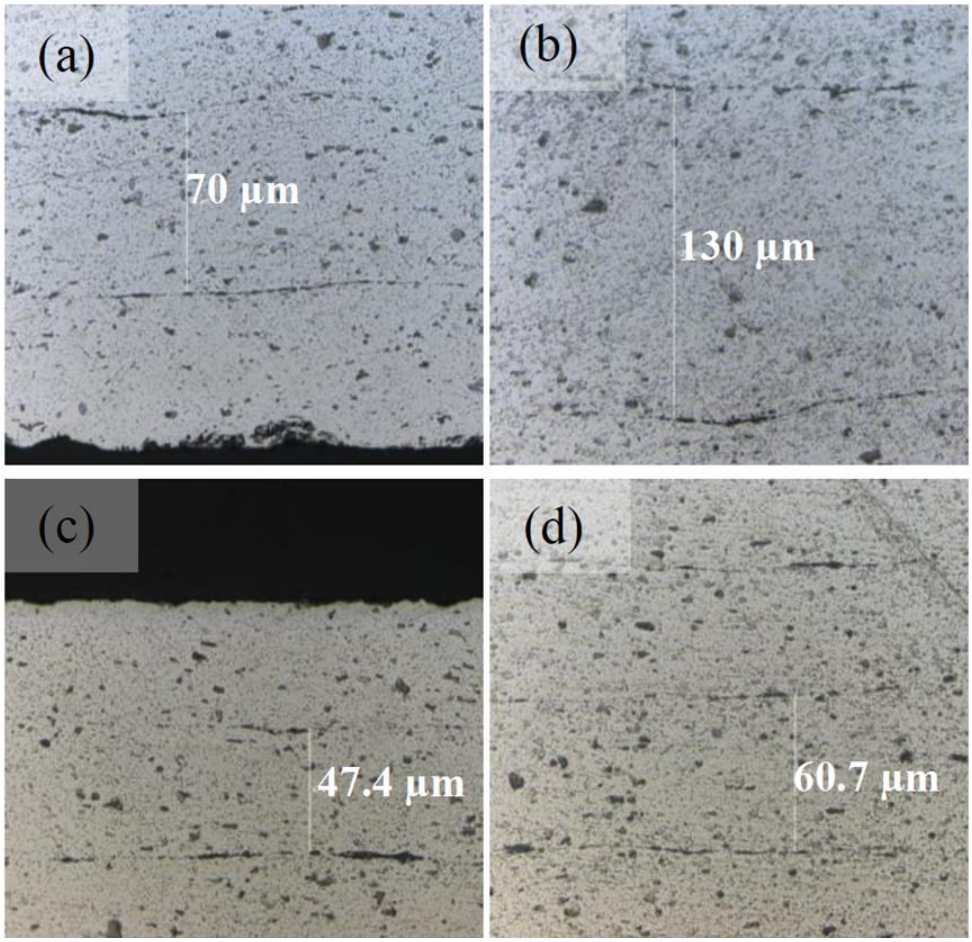

Fig.3.1: Optical Microscope microstructures from a 4-ARB sample periphery layer (a), one middle layer (b) and from a 5-ARB sample a periphery layer (c) and middle layers (d).

3.1.2 Raman Spectroscopy

To further characterize the interface lines observed by the optical microscope several Raman spectroscopy measurements were carried out. Fig.3.2 shows a photo (a) of a sample interface region that was analysed through Raman imaging in the area contained by the red square in the photo. The Raman maps corresponding to the regions of interest corresponding to the Al_xO_y and GO peaks in the spectra are shown in Fig.3.2 (b). The peaks of D and G bands for the GO are at 1352 cm-1 and 1568 cm^{-1} respectively, which are both typical for pristine GO [9]. A peak of an Al oxide (Al_xO_y [22]) appears at 698 cm^{-1}. The Al oxide formation was expected and can be explained by the presence of air during the pre-heating process or H_2O from the GO suspension. Intensity

maps show that in this region GO is more abundant than Al_xO_y and the presence of GO clusters can be related to a possible non-homogenous distribution of the reinforcement.

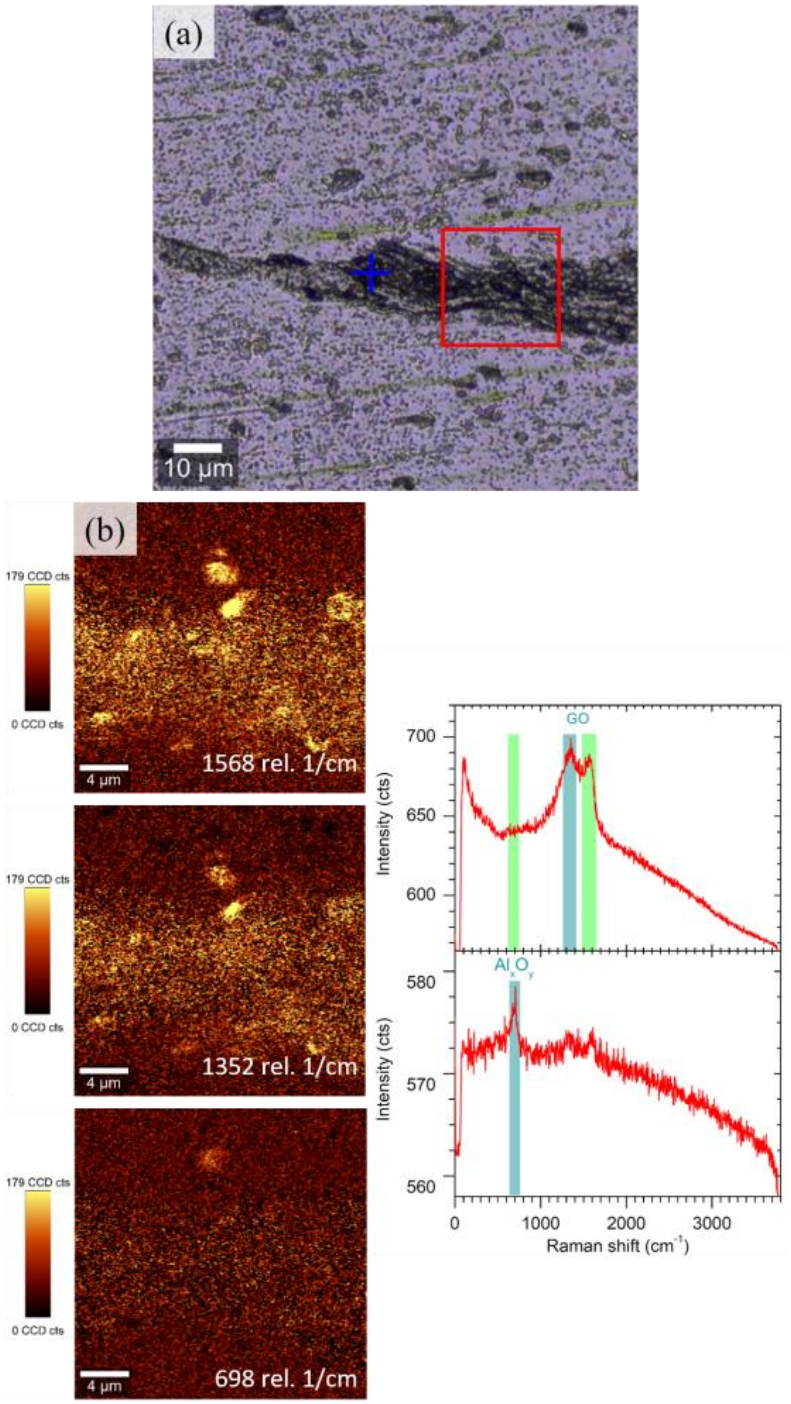

Fig.3.2: Mapped region of an interface (a) and its Raman spectra and intensity maps (b).

Focusing on another interface region of the same sample, shown in the microscope photo of Fig. 3.3 (a), 8 Raman spectra were taken along the red line marked over the photo and all depicted in the graph of Fig. (b). The colours of the spectra match the colours of the crosses marked along the red line as they represent the positions at which the spectra were recorded. Note that in the orange spectrum it is possible to identify the specific spectral signatures of Al_xO_y peaks matching the brighter region of the interface, whereas the GO peaks match the darker regions. Although the peaks for D and G bands of GO should be approximately the same intensity, this is not seen in the red spectrum. Since several defects can influence D band peak values, this discrepancy can be explained by harsh oxidization of the GO reinforcement.

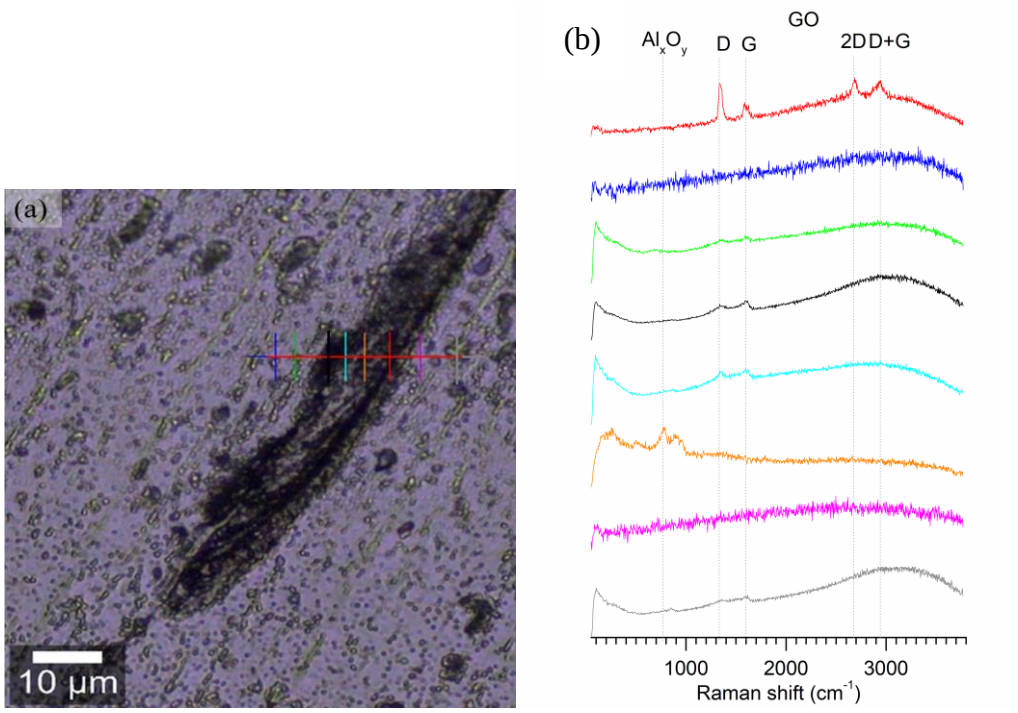

Fig.3.3: Raman Spectra (b) corresponding to the points marked along the red line in the microscope image.

3.1.3 SEM results

An interface where some material was removed by the polishing process was observed in SEM and shown in Fig. 3.4. The formed Al_xO_y can be observed in the middle of the interface (b) whereas the GO cannot be identified neither quantified.

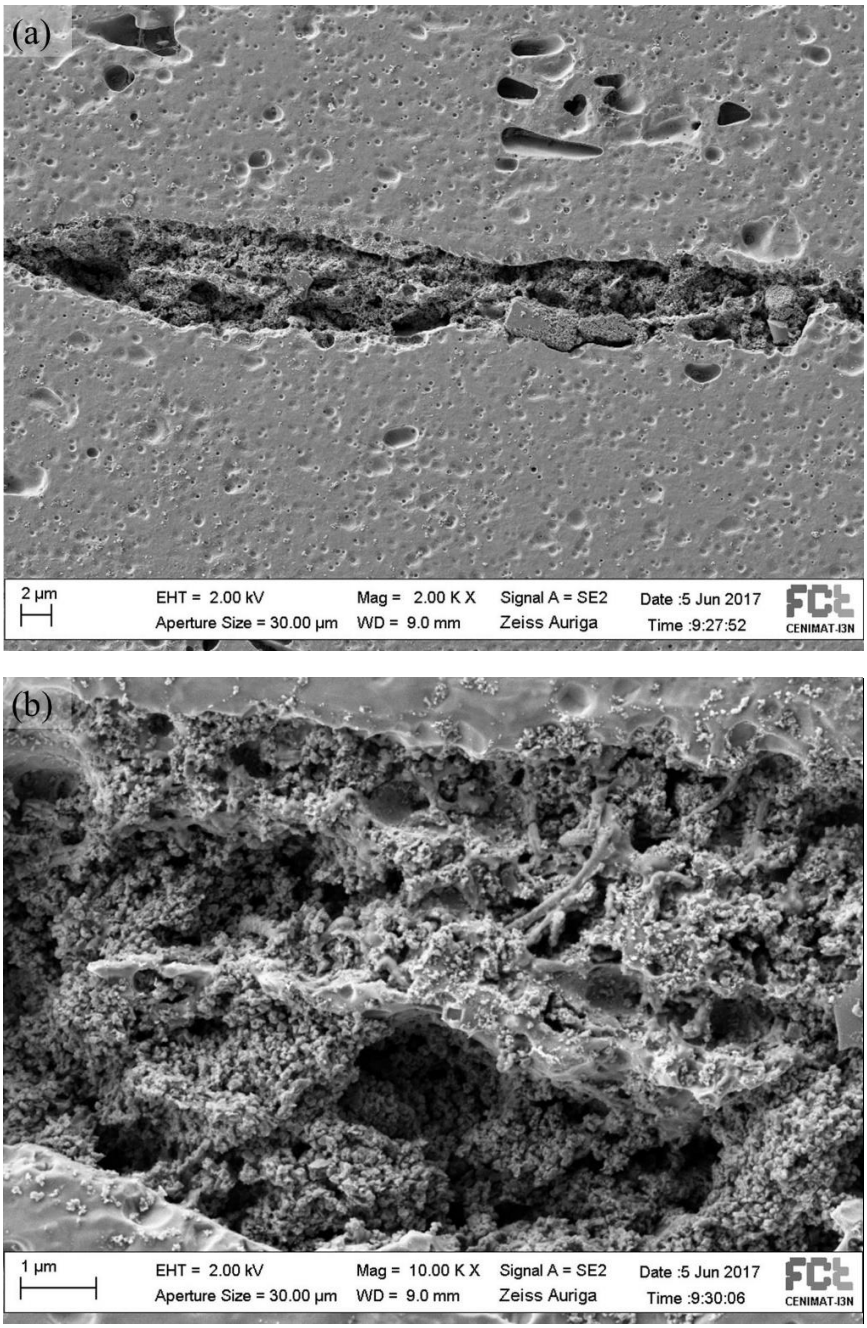

Fig.3.4: SEM micrographs of an interface belonging to a 5-ARB sample at lower (a) and higher (b) magnification.

3.2 Mechanical Results

3.2.1 Microhardness Test

ARB processed materials have an increment on its hardness. For the earlier ARB cycles this increase is primarily related to strain hardening (i.e., increase in density of dislocations and their interactions) following by subgrain boundaries and/or dislocation cell wall formation [5]. The influence of grain refinement is attributed at higher ARB cycles [20].

The average microhardness values of the ARB processed samples are shown in Fig.3.5. The results were obtained for 4 or 5-cycle ARB at different concentrations and at both TD and RD sections. For the RD section, the hardness is higher in all tested samples as along this direction the sample suffers a greater plastic deformation when rolled which can be observed at a macroscopic level. The microhardness gap between TD and RD is ~5% in all samples, which confirms that ARB processed materials are anisotropic. GO influence on the average hardness (4-cycle ARB and both directions) is ~10%. On average, when comparing the influence of the 5th cycle, the results show a significant increase of ~14 %, which is related to grain refinement caused by the 5th cycle. Considering all of the reinforced samples at 4-cycle ARB, the one with higher microhardness values is the lowest in terms of concentration (0.5 mg/ml, ~75 HV) and both 2.5 mg/ml and 10 mg/ml samples have similar results (~71 HV and ~70 HV, respectively). This difference can be explained by a better adhesion and consolidation between the Al layers on the samples with less reinforcement. However, when the GO was applied by airgun-spraying, the suspension volume was not accounted for, so the exact quantity of graphene cannot be quantified and for the 5-cycle samples (0.5 mg/ml and 2.5 mg/ml concentrations) the microhardness values have no significant difference (~83 HV and ~82 HV respectively).

For the annealed Al sample the microhardness values for the TD and RD sections are 40.75 HV and 41.75 HV respectively. This means that the four ARB cycles promoted an increase of ~57 % on its microhardness.

Fractures on the Al matrix and the presence of Aluminium oxide, observed in Raman spectroscopy and SEM, also influence the hardness of the samples.

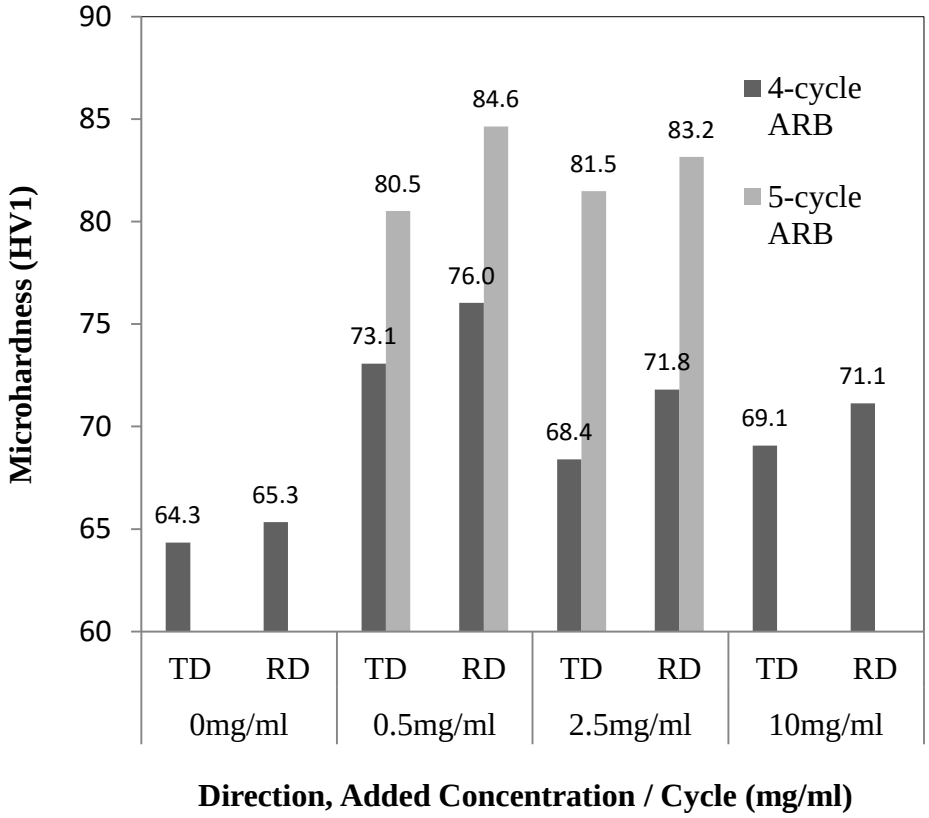

Fig.3.5: Average microhardness comparison between the GO concentrations of the suspension applied, direction and number of ARB cycles.

The hardness profiles of two samples using the same concentration (2.5 mg/ml) and same direction section (RD) but different number of ARB cycles are represented in Fig.3.6. As expected, these profiles are not linear but become an oscillatory form since the plastic deformation is not homogenous through the thickness of the sample and through each layer. The standard deviation and variance values for the 4-cycle ARB sample are 4.4 HV and 19.3 HV^2, respectively. For the 5-cycle ARB sample the standard deviation and variance are 3.3 HV and 10.8 HV^2, respectively. As referred to before, this difference exists because the grain refinement is more homogenous in the 5-cycle ARB sample than the 4-cycle sample. As the number of ARB cycles increase, it is expected that the standard deviation and variance decrease, and when the hardening behaviour saturates at larger strains, these values are reduced to zero, as previously reported [20].

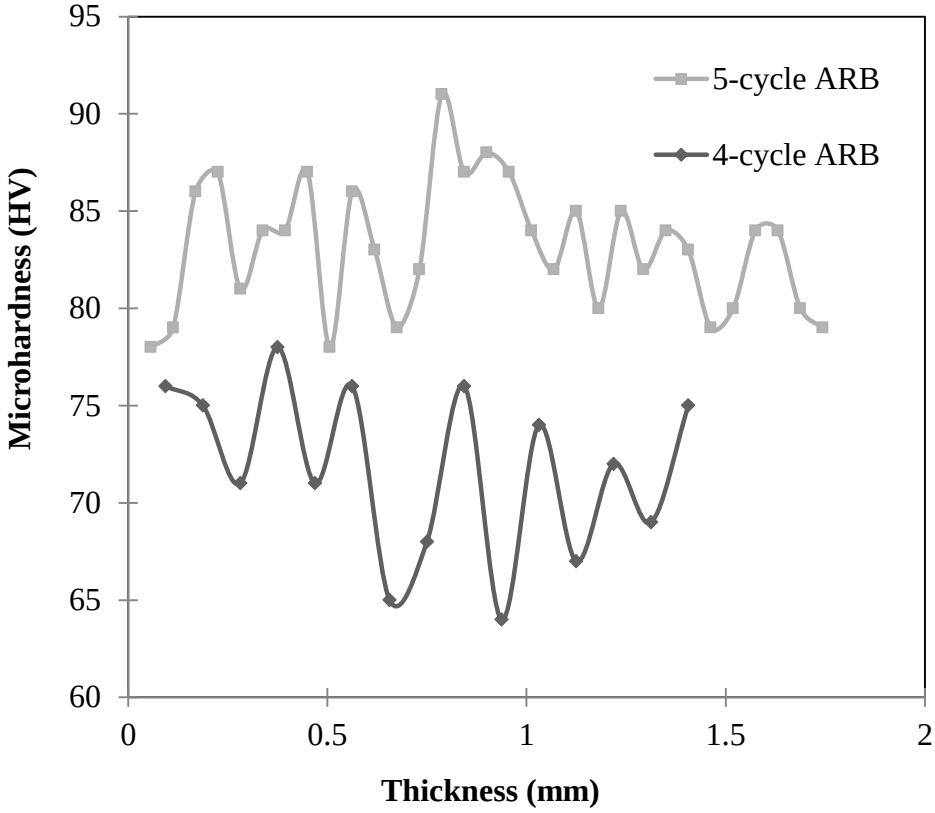

Fig.3.6: Two microhardness profiles of identical samples but different number of ARB cycles (4 and 5).

3.2.2 Three-point bending test

The three-point bending test was performed in order to observe the behaviour of the samples when subjected to significant tensile and compressive stresses. The processed composites that were reinforced using the highest GO concentration (10 mg/ml) and the 5-cycle using 0.5 mg/ml concentration could not be tested since delamination occurred during the cutting process, revealing a weak bond between layers for these specimens. The results concerning the stiffness modulus under bending conditions for the tested samples are represented in Fig. 3.7. Note that, according to Eq. (1), these values should be independent from the dimensions of the sample and length of the support span. The influence of the GO reinforcement is clearly present since for the same number of ARB cycles (4) the composites revealed E_B ~82% higher than the sample with no reinforcement. The weaker performance of the 5-cycle ARB composite results from a complete delamination, shown in Fig.6.2, which occurred at a stress of 105 MPa, suggesting that, for this specimen, the bond between layers was weaker than the 4-cycle samples, since no delamination was visible in any of them. For the same sample, there

is no significant difference when considering the tested directions. The ARB process also influenced the bending strength due to strain hardening (severe plastic deformation) and grain refinement, although not as much as the GO reinforcement. In Fig. 3.8 are represented the yield strength of the samples. For the 4-cycle ARB, aluminium yield strength was not achieved due to the load cell limitations (500 N) since the length of the support span was 20 mm (instead of 30 mm) and more applied force was needed to reach plastic range.

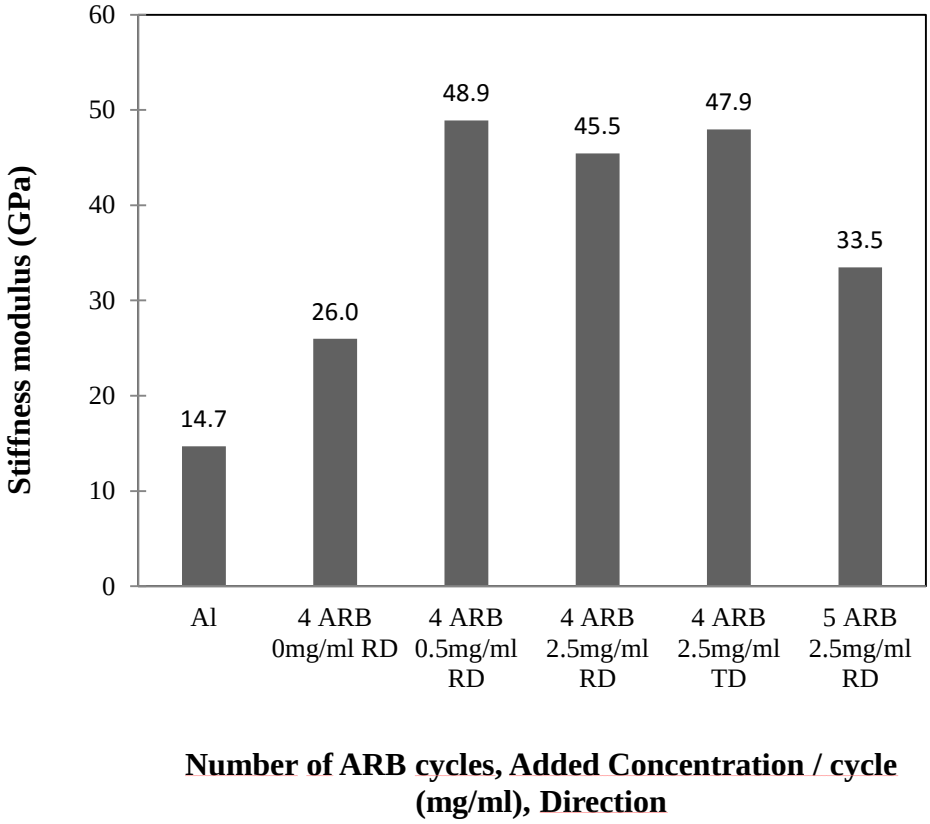

Fig. 3.7: Comparison of the stiffness modulus values measured during bending between GO concentrations of the suspension applied, direction and number of ARB cycles.

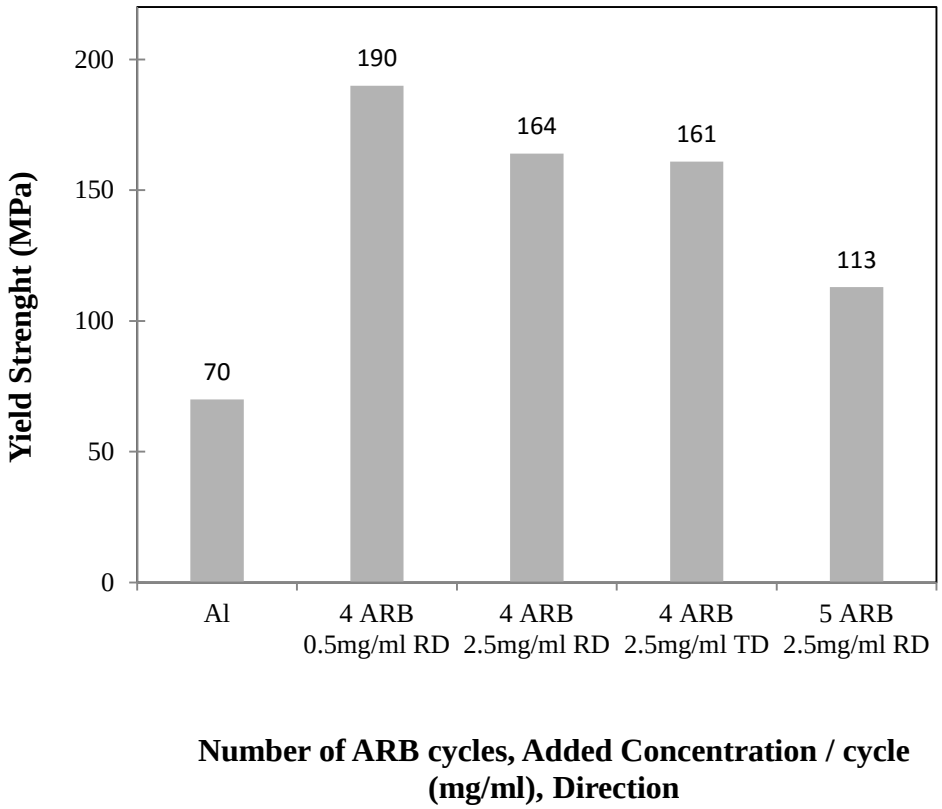

Fig. 3.8: Yield strength comparison between GO concentrations of the suspension applied, direction and number of ARB cycles.

Overall and considering this test, the 4-cycle ARB composite using the lowest concentration of reinforcement (0.5 mg/ml) had the best performance which is similar to the microhardness results for this number of ARB cycles.

3.3 Electrical Conductivity

To complement the characterization of the composites, two different electrical conductivity tests were carried, since electrical conductivity in metals and MMCs could be a deciding factor depending on the application. The results conducted by Eddy current tests are presented and compared in Fig. 3.9. As expected, the annealed Al sample achieved better results (~55 % IACS) when compared to others due to the presence of aluminium oxide and GO on them. As the number of ARB cycles increase, the conductivity decreases since the 5-cycle ARB samples have double the Al layers and therefore double the oxide layers. Except for the 0.5 mg/ml sample, the 4-cycle composites have an inferior conductivity than the sample without reinforcement given the insolating properties of GO.

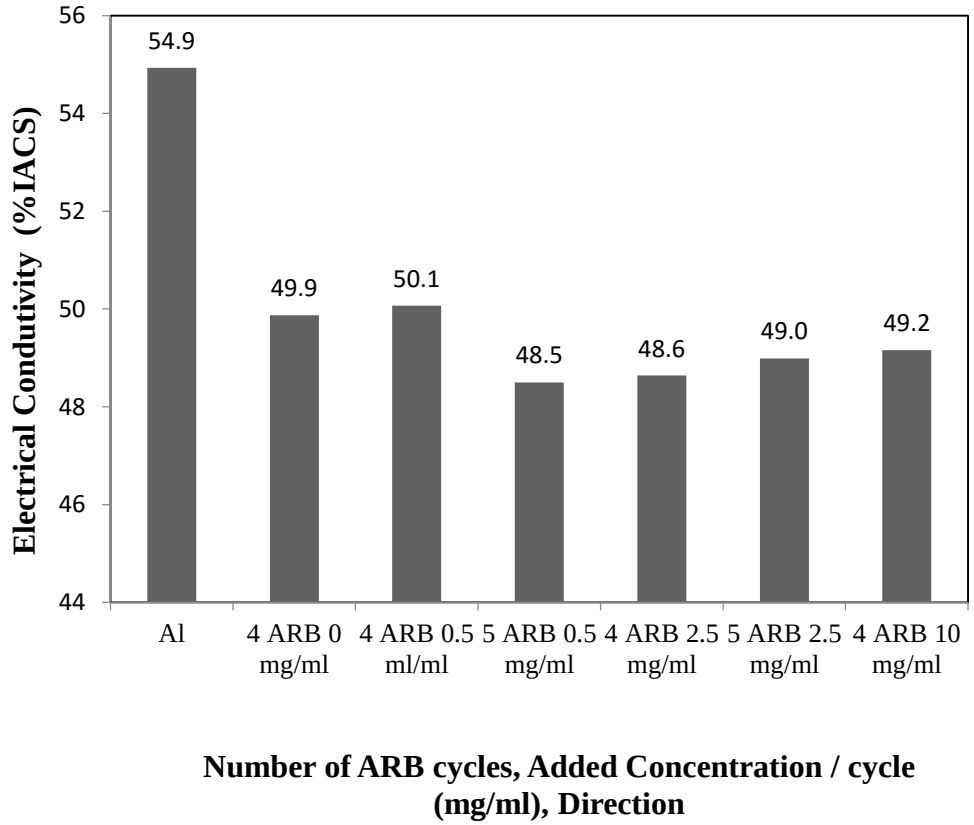

Fig. 3.9: Electrical conductivity (% IACS) carried out by Eddy Current tests comparison between GO concentrations of the suspension applied, direction and number of ARB cycles.

Since internal fractures and delamination also influence the electrical conductivity, the better results revealed by the composite using the smallest concentration when compared with the sample without reinforcement can be explained by a better adhesion between layers and its structure having less defects or inferior aluminium oxide presence on its layers' interface.

For comparison, the 4 point probe resistivity measurements are displayed in Table 6.3 (Appendix 6) and were converted to % IACS which are presented in Fig. 3.10. The processed samples revealed a much more significant electrical conductivity decrease in this test when comparing with the Eddy Current results. According to the different geometries of the conduction paths which characterize the two tests (in-depth conduction in the 4-point probe measurements vs. superficial conduction channels in the Eddy current measurements), it is to be expected that the 4-point test will be more sensitive to the anisotropic characteristics of the processed material, which in turn are exacerbated as the number of ARB cycles is increased. Thus, the lesser observed decay in the conductivity measured by the Eddy current method can be understood.

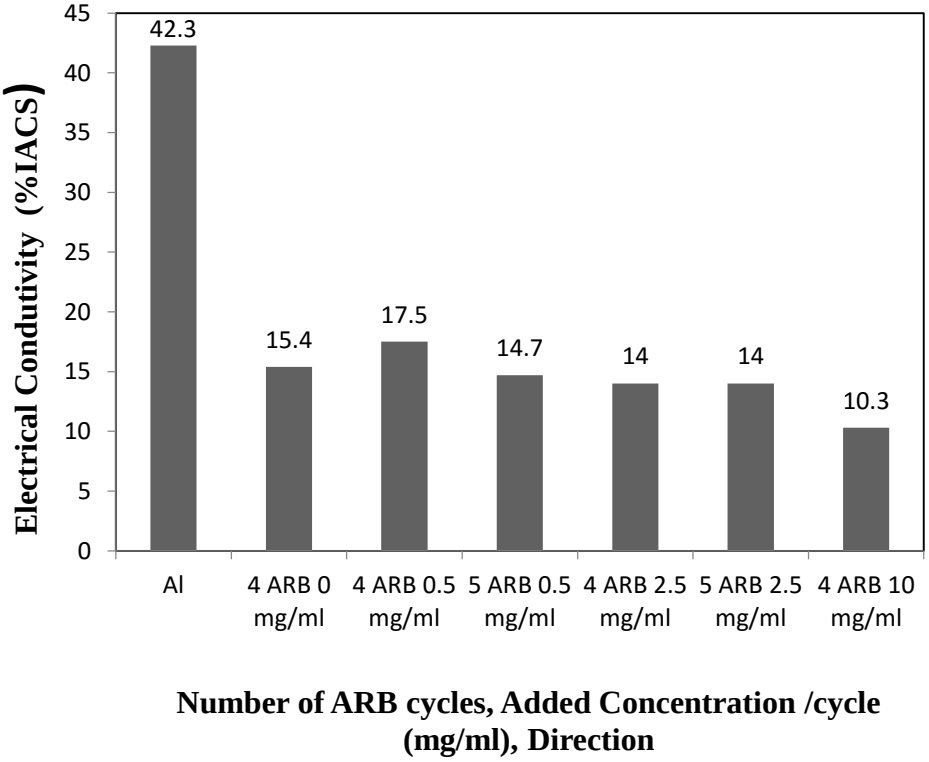

Fig. 3.10: Electrical condutivity carried out by 4 point probe tests comparison between GO concentrations of the suspension applied, direction and number of ARB cycles.

According to the thickness of the samples (Table 6.2) the resistivity calculation followed Eq. (2) except for the Al sample which followed Eq. (3). The 4-cycle ARB using 0.5 mg/ml GO revealed once again a superior electrical conductivity than the 4-cycle Al sample (~2 % IACS). The sample which revealed the worst electrical conductivity was the one using the highest concentration (10 mg/ml) applied. This is probably related to the fact that this sample was slightly bent during the rolling process, which might have influenced the measurement of the 4 point probe, or related to internal delamination or fractures and the concentration of both oxides (Al_xO_y; GO).

4 Conclusions

Ultrafine structured Aluminium GO-reinforced with GO composite was produced by ARB up to 5 cycles. In order to achieve UFG across the thickness of the samples, it was intended to produce samples up to 6 ARB cycles, however, it was not possible due to the rolling mills' power limitation. Since each ARB cycle promotes a 50% reduction of the stacked Al layers, it was expected that the thickness of the samples was equal to the original Al sheet (0.8 mm) regardless of the number of ARB cycles. As can be seen in Table 6.2, this thickness values were not achieved due to a protection clearance of ~1 mm of the rolling mills. Microstructural, mechanical and electrical characterizations were carried out on several samples with different concentrations of the applied GO and number of cycles and compared with each other. The conclusions drawn from the results can be summarized as follows.

Using airgun-spraying to deposit the GO reinforcement revealed to be a good method although it is difficult to guarantee a perfect deposition free of irregularities at this scale.

Optical Microscope (OM) results show that the deformation of the layers is not homogenous across the sample for this number of ARB cycles. Middle layers (earlier ARB cycles) suffer less deformation than the periphery ones, although this difference tends to decrease at later ARB cycles.

The presence of GO has been identified by Raman spectroscopy where its D and G were well identified and mapped though the Al junction. Some small regions of Al_xO_y were also identified both by Raman mapping and EDS/SEM.

The presence of GO contributed to an increase of ~10% to the average microhardness. Concerning the 4-cycle ARB samples, the lowest concentration suspension (0.5 mg/ml) revealed to increase the microhardness the most and it is presumably related to a more homogenous deposition. The fifth ARB cycle contributed to a ~14% increase on the microhardness of the tested samples. The anisotropy of the ARB samples was confirmed since the microhardness average of the RD sections is ~5% superior to the TD sections in all samples due to a higher grain refinement along the rolling direction. Hardness profiles present an oscillatory form at this number of cycles which tends to become linear as the number of ARB cycles increase.

Bending tests revealed a greater influence of the GO reinforcement over the bending stiffness than the number of ARB cycles. Complete delamination only occurred in the 5-cycle ARB hence its low performance in this test.

In contrast with the mechanical results, in which the GO composites revealed a great improvement in relation to the annealed aluminium, electrical conductivity decreased for the processed ARB samples. This electrical conductivity loss was expected given the insulator properties of the aluminium oxide and GO. Depending on the application for this material, this loss may not be a decisive factor given the observed mechanical improvements.

On a personal note, I am really pleased and proud of this work, not only because the achieved results revealed that a cheap and abundant metal like aluminium can have its properties greatly improved, resulting in a wider range of its applications, but also for all the knowledge that I acquired during this dissertation by reading several articles and learning how to work with laboratory equipment like the rolling mills, precise cutting machine, optical microscope and its software (LAS), microhardness machine, universal testing machine and its software (Trapezium).

5 References

1. António, J., Fonseca, M.: Produção e Caracterização de Compósitos de Alumínio Reforçados com Nanotubos de Carbono. 9 (2012).
2. Ana, S.V.A., Reihanian, M., Lotfi, B.: Accumulative roll bonding (ARB) of the composite coated strips to fabricate multi-component Al-based metal matrix composites. Mater. Sci. Eng. A. 647, 303–312 (2015).
3. Huang, Y., Langdon, T.G.: Advances in ultrafine-grained materials. Mater. Today. 16, 85–93 (2013).
4. Daneshvar, F., Reihanian, M., Gheisari, K.: Al-based magnetic composites produced by accumulative roll bonding (ARB). Mater. Sci. Eng. B Solid-State Mater. Adv. Technol. 206, 45–54 (2016).
5. Gashti, S.O., Fattah-alhosseini, A., Mazaheri, Y., Keshavarz, M.K.: Effects of grain size and dislocation density on strain hardening behavior of ultrafine grained AA1050 processed by accumulative roll bonding. J. Alloys Compd. 658, 854–861 (2016).
6. Lee, S.H., Sakai, T., Shin, D.H.: Fabrication of ultrafine grained aluminum by differential speed accumulative roll-bonding (ARB) process. Mater. Trans. 44, 1382–1385 (2003).
7. Schmidt, C.W., Knieke, C., Maier, V., Höppel, H.W., Peukert, W., Göken, M.: Accelerated grain refinement during accumulative roll bonding by nanoparticle reinforcement. Scr. Mater. 64, 245–248 (2011).
8. Garcia Maraschin, T.: Preparação De Óxido De Grafeno E Óxido De Grafeno Reduzido E Dispersão Em Matriz Polimérica Biodegradável Dissertação Para a Obtenção Do Título De Mestre Em Engenharia E Tecnologia De Materiais. 89 (2016).
9. Wang, J., Li, Z., Fan, G., Pan, H., Chen, Z., Zhang, D.: Reinforcement with graphene nanosheets in aluminum matrix composites. Scr. Mater. 66, 594–597 (2012).
10. Zaaba, N.I., Foo, K.L., Hashim, U., Tan, S.J., Liu, W.W., Voon, C.H.: Synthesis of Graphene Oxide using Modified Hummers Method: Solvent Influence. Procedia Eng. 184, 469–477 (2017).
11. Edwards, R.S., Coleman, K.S.: Graphene synthesis: relationship to applications. Nanoscale. (2013).
12. Santosh, S., Bhanureka: Graphene based piezo resistive sensor fabrication and its characterization. In: Second Internationa Conference on Recent Advances in Science & Engineering-2015 (2015).
13. Strudwick, A.J., Weber, N.E., Schwab, M.G., Kettner, M., Weitz, R.T., Wunsch, J.R., Mullen, K., Sachdev, H.: Chemical Vapor Deposition of High Quality Graphene Films from Carbon Dioxide Atmospheres. ACS Nano. (2015).
14. Ding, J.N., Liu, Y.B., Yuan, N.Y., Ding, G.Q., Fan, Y., Yu, C.T.: The influence

of temperature, time and concentration on the dispersion of reduced graphene oxide prepared by hydrothermal reduction. Diam. Relat. Mater. (2012).

15. Badhulika, S., Terse-Thakoor, T., Villarreal, C., Mulchandani, A.: Graphene hybrids: synthesis strategies and applications in sensors and sensitized solar cells. Front. Chem. (2015).
16. Wong, C.H.A., Sofer, Z., Kube ova, M., Ku era, J., Mat jkova, S., Pumera, M.: Synthetic routes contaminate graphene materials with a whole spectrum of unanticipated metallic elements. Proc. Natl. Acad. Sci. (2014).
17. Nasrollahzadeh, M., Babaei, F., Fakhri, P., Jaleh, B.: Synthesis,characterization, structural, optical properties and catalytic activity of reduced graphene oxide/copper nanocomposites. RSC Adv. (2015).
18. Shamaila, S., Sajjad, A.K.L., Iqbal, A.: Modifications in development of graphene oxide synthetic routes, (2016).
19. Faria, P., Duarte, P., Barbosa, D., Ferreira, I.: New composite of natural hydraulic lime mortar with graphene oxide. Constr. Build. Mater. 156, 1150–1157 (2017).
20. Eizadjou, M., Manesh, H.D., Janghorban, K.: Microstructure and mechanical properties of ultra-fine grains (UFGs) aluminum strips produced by ARB process. 474, 406–415 (2009).
21. Smits, F.M.: Measurement of Sheet Resistivities with the Four-Point Probe. Bell Syst. Tech. J. (1958).
22. Thomas, P. V., Ramakrishnan, V., Vaidyan, V.K.: Oxidation studies of aluminum thin films by Raman spectroscopy. Thin Solid Films. 170, 35–40 (1989).

6 Appendixes

Table 6.1: Geometric factor F(t/s) values for different t/s ratios, adapted from [21]**.**

t/s	*F(t/s)*
0.4	0.9995
0.5	0.9974
0.5555	0.9948
0.6250	0.9898
0.7143	0.9798
0.8333	0.9600
1.0	0.9214
1.1111	0.8907
1.25	**0.8490**
1.4286	0.7938
1.6666	0.7225
2.0	0.6336

Table 6.2: Thickness values of the produced and tested samples.

Sample	Thickness (mm)
Al	0.8
4 ARB 0 mg/ml	1.8
4 ARB 0.5 mg/ml	1.5
5 ARB 0.5 mg/ml	1.8
4 ARB 2.5 mg/ml	1.5
5 ARB 2.5 mg/ml	1.8
4 ARB 10 mg/ml	1.5

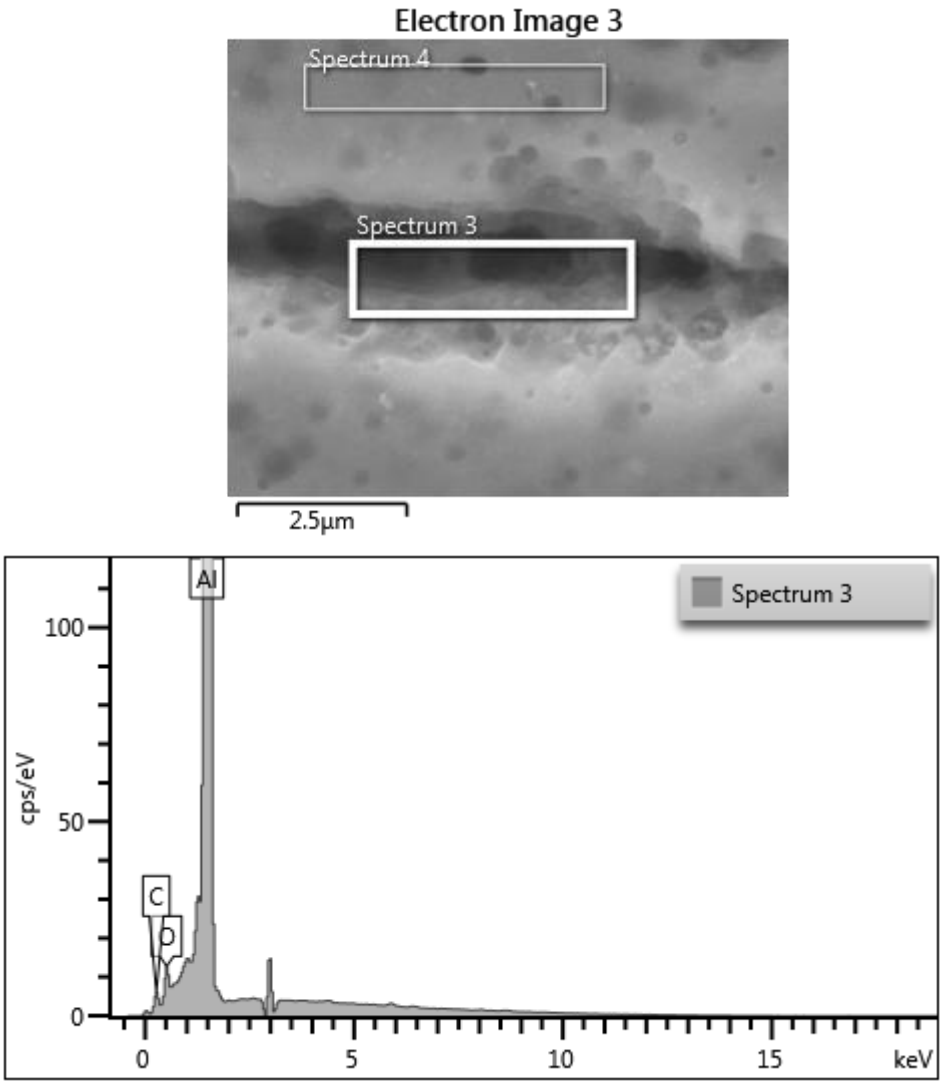

Fig. 6.1: EDS mapping of the interface observed in Fig.3.4 from a 5-cycle ARB sample.

Table 6.3: Electrical conductivity and resistivity values obtained by Eddy Current and 4 point probe tests of the tested samples.

Sample	Eddy Current (% IACS)	4 point probe resistivity (ohm.m)
Al	54.93	4.07891E-08
4 ARB 0 mg/ml	49.87	1.12053E-07
4 ARB 0.5 mg/ml	50.07	9.88015E-08
5 ARB 0.5 mg/ml	48.5	1.16934E-07
4 ARB 2.5 mg/ml	48.64	1.23389E-07
5 ARB 2.5 mg/ml	48.99	1.23389E-07
4 ARB 10 mg/ml	49.16	1.67932E-07

Fig.6.2: Observed delamination of the 5-cycle ARB sample caused by the three-point bending test.